Sparsity- based GPR blind deconvolution and wavelet estimation

Alaeddin Ebrahimi⋆, Ali Gholami and Majid Nabi-Bidhendi
Institute of Geophysics, university of Tehran, Tehran, Iran
⋆Corresponding author: ala_ebrahimy@ut.ac.ir

ABSTRACT
Improving the vertical resolution of Ground Penetrating Radar (GPR) data by blind deconvolution technique is an approach we target here. Sometimes geologic situations such as presence of clay or humidity lead to blurred sections. Advanced processing steps, that are so common in seismic reflection, such as deconvolution are needed. In this approach the sparse deconvolution algorithm on GPR data has been used in a novel way. It is often assumed that reflectivity series are sparse and noise is random. Generalized Cross Validation (GCV) method has been used to estimate the desired wavelet and to find the optimum iteration in the deconvolution algorithm. To examine the efficacy of the method, it is applied to synthetic data. The GCV and MSE curves versus iteration are then plotted in order to determine the optimal point. The final deconvolved section shows a satisfying result for GPR field data and the speed and accuracy of this robust algorithm to reconstruct reflectivity series is considerable.

Key words: Ground Penetrating Radar (GPR), Blind deconvolution, Sparsity, Generalized Cross Validation(GCV) and Reflectivity series.

INTRODUCTION

Ground penetrating radar (GPR),amongst all near-surface geophysical techniques, isone of the most commonly applied non- invasive subsurface characterization tools for engineers (Benedetto, 2002; Hugenschmidt, 2002), archeologists (Goodman, 1994; Sternberg and McGill, 1995), geologists (Bano et al., 2000; Bednarczyk and Szynkiewicz, 2015) and other related tasks. A GPR tool has different parts, each of which is responsible for some function. The transmitter and the receiver are the main ones. A transmitter sends electromagnetic waves into the earth in the frequency range of 10 MHz to 2 GHz and a receiver detects them after travelling back from the earth (Jol, 2008).

The basic processing steps are the same asseismic processing and significant insights into GPR processing can be gained from developments of the period (Jol and Bristow, 2003). However, there are some key differences between them, which are important for validity of more advanced processing methods (Baker et al., 2001). Attenuation and dispersion effects are more extreme with GPR, and therefore, the frequency component (and phase equations) of signals can change markedly with recorded time and depth (Jol, 2008). Unfortunately, many of the advanced signal processing and analysis methods used in GPR data interpretation are poorly suited for use in near-surface environments, primarily because of the limiting assumptions inherent in their mathematical descriptions (e.g. high frequency, uniform half-space sub-surfaces, etc.) (Daniels, 2004).

Deconvolution is a temporal inverse filtering technique that improves resolution of data (Yilmaz, 2001) by compressing the measured GPR wavelet into a distinct form. On the other hand, it is applicable to remove effect of source wavelet from acquired data (Neves et al., 1995) and just leaves an impulse response of underground layers. While deconvolution is considered to be a key step in seismic processing (e.g. Yilmaz, 2001), in GPR data, these are very restricting conditions as the subsurface is more complex and propagating GPR wavelet is totally vectored with non-planer, spatially complex fields (Conyers and Goodman, 1997). This has led to a debate on the usefulness of casual deconvolution techniques.

The features and considerations of GPR reflection data closely depend on optimized temporal resolution of sections. However, unprocessed GPR data appears blurred and incorrectly images true reflectivity series due to real characteristic of the GPR wavelet (Van Dam and Schlager, 2000).

Deterministic deconvolution has been applied to GPR data by Xia et al., (2003, 2004) and approximately 50 % improvementin the temporal resolution of the section has been presented (Xia et al., 2003). The wavelet in deterministic deconvolution has been earned by measuring the signal traveling through the air while keeping the source and receiver antennas in front of each other (Economou and Vafidis, 2011). There are some techniques to estimate source wavelet, published in literatures (Amundsen, 2001). Air wave that has occurred because of antennaseparation and especially first waveform status could be used as a GPR wavelet (Gottsche et al., 1994). In another way, a plate sends electromagnetic pulse and another plate that has faced it, records a wavelet (Xia et al., 2004) while measured wavelet is not available every time as it is time consuming and difficult technically.

A type of blind deconvolution method has been applied to GPR data by Schmelzbach et al., (2011) where parameterization of wavelet has been designed as convolution of a wavelet with a dispersive all pass filter, including prior information about wavelet to be estimated in a Bayesian framework and linked with the assumption of a sparse reflectivity. This method has earned increased temporal resolution compared to the results of standard processing (Schmelzbach et al., 2011). Chahine et al., (2009) cast the convolution model as multidimensional data which accomplishes blind deconvolution through independent component analysis. They carried out the GPR for pavement evaluation. According to Chahine et al., (2009), the blind deconvolution technique could be used as a method to retrieve the latter reflectivity series and recover time resolution without reliance on prior information. Clearly, a nonlinear contrast function has been selected which fits to the sparse quiddity (the inherent nature) of the reflectivity series. Moreover, Li (2014) extends the classical minimum entropy deconvolution strategy and forms ageneral-purpose framework of blind deconvolution of GPR data, according to which the formulation of sparsity-promoted optimization problem in a scale-invariant regularizer has been suggested. The substituted iterative method is defined to solve the by-product, non-convex optimization issue. Rudimentary consequences show that by applying this method to GPR data, vertical resolution will be improved. Recently, Schmelzbach, and Huber (2015) presented a method of GPR deconvolution wherein, first a signal-by-signal minimum-phase deconvolution was applied and then, a global phase rotation was applied to maximize the sparseness of the minimum-phase deconvolved data where as some series have needed for a better sparseness estimation and steady phase rotation.

In this paper, the blind deconvolution scheme is used to estimate the wavelet and reflectivity series in an alternating fashion using sparse analysis tools. The solution procedure is fully automated so that the regularization parameter is determined by the generalized cross validation (GCV) score. In what follows, we first present the theory of our blind deconvolution and then the synthethic data examples are tested and the method is applied to GPR field data.

Theory of blind deconvolution

GPR trace can be represented as a convolution of source wavelet with the earth reflectivity series and additive noise (Daniels, 2004; Giannopoulos, 2005; Irvin and knight, 2006)

$$w * r + e = y \tag{1}$$

where r is the reflectivity series, a column vector of length N, w is the source wavelet of length M, $*$ denotes convolution operator, y is the GPR trace which is contaminated by additive random noise **e**. Equation (1) can be rewritten in matrix form as

$$y = Wr + e = Rw + e \tag{2}$$

Where R, W $\in$ R$^{n \times n}$ are square Toeplitz matrices with kernels r and w respectively.

Since both W and R are unknown, we solve Equation (2) in a sequential form by first estimating **w** and then using the estimated wavelet to solve the problem for **r**. In the following sections each step is described in details.

Wavelet and reflectivity series estimation

A wavelet can be recovered from equations (3) and (4).

$$\mathbf{F\hat{w}} = \operatorname{argmin} \|\mathbf{Fy} - \mathbf{w}\|_2^2 + \lambda \|\mathbf{D}^{(2)}\mathbf{w}\|_2^2 \tag{3}$$

Where $D^{(2)}$ is the second order differential operator, F is the Fourier transform matrix, $\hat{\mathbf{s}} = \mathbf{Fs}$ for a given vector **s**, $\|s\|_p^p = \Sigma_i s_i{}^p$ and $\lambda > 0$ is a regularization parameter. Solving

$$\hat{\mathbf{w}} = \mathbf{F}^T(\mathbf{I} + \lambda \mathbf{D}^{(2)^T} + \mathbf{D}^{(2)})^{-1}\mathbf{Fy} \tag{4}$$

Where **I** is the identity matrix.

Using the initial wavelet $w^{(l)}$ estimated by equation (4), averaged over all traces, and setting $l = 1$, a sparse reflectivity section can be obtained by nonlinear optimization (5) which is applied for each trace separately

$$\mathbf{r}^{(\ell)} := \operatorname{argmin}_r \|\mathbf{r}\|_1 \text{ subject to } \|\mathbf{y} - \mathbf{w}^{(\ell-1)} * \mathbf{r}\|_2^2 \leq \gamma \tag{5}$$

Then the estimated section is used to update the source wavelet in a least square form while fixing the support of the wavelet. The process is repeated until convergence. Equation (5) is solved via the Bregman iteration summarized below (see Gholami and Sacchi (2012) for more details about the algorithm).

$$\text{Set: } D = \operatorname{diag}\left(\frac{1}{\alpha|\hat{w}|^2 + \beta}\right)$$

$$\text{Initialize: } k = 0, \mathbf{d}^0 = \mathbf{b}^0 = 0$$

$$\text{while } \|\mathbf{W}\hat{\mathbf{x}}^k - \hat{\mathbf{y}}\|_2^2 > \gamma$$

$$\hat{\mathbf{x}}^{k+1} = \mathbf{D}(\alpha \mathbf{W} * \hat{\mathbf{y}}^k + \beta \mathbf{F}[\mathbf{d}^K - \mathbf{b}^k])$$

$$\mathbf{d}^{k+1} = \operatorname{prox}_{1/\beta}^1(\mathbf{F}^{-1}\hat{\mathbf{x}}^{k+1} + \mathbf{b}^k)$$

$$\mathbf{b}^{k+1} = \mathbf{b}^k - [\mathbf{d}^{k+1} - \mathbf{F}^{-1}\hat{\mathbf{x}}^{k+1}]$$

$$\hat{\mathbf{y}}^{k+1} = \hat{\mathbf{y}}^k + \hat{\mathbf{y}} - \mathbf{w}\hat{\mathbf{x}}^{k+1}$$

$$k = k + 1$$

End while
$$\mathbf{r} = \mathbf{d}^k$$

In the algorithm, we have tested numerous values of α and β and finally $\alpha = 0.5$, $\beta = 1$ derived successfully which meet suggested values by Gholami and Sacchi (2012). Defined Prox function is
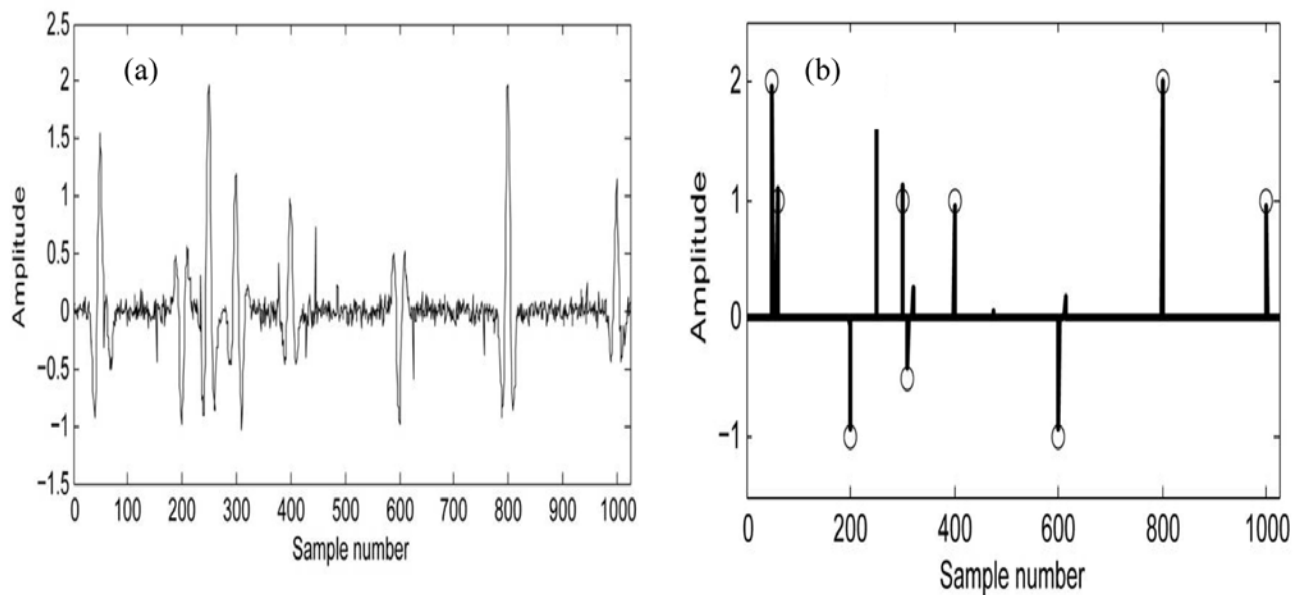
Figure 1. (a)Synthetic trace , (b)estimated and original reflectivity series showed with circles.

$$\text{prox}_\tau^1 = \text{sign}(y)\max\left(|y| - \tau, 0\right) \tag{6}$$

Generalized Cross Validation (GCV) score is used (Golub et al., 1979) to find the optimum number of iterations (Gholami and Sacchi, 2012)

$$\text{GCV(k)} = \frac{\left\| y - W d^k \right\|_2^2}{\left[N - c.\text{nnz}(d^k) \right]^2} \tag{7}$$

Where N is number of data in each trace, c is stabilizing parameter and nnz is non-zero elements of a vector.

Numerical Examples

Accepted waveform for GPR signals was mainly supposed to be a Ricker wavelet (Daniels, 2004;Giannopoulos, 2005; Irvin and knight, 2006). The Ricker wavelet (Ricker, 1953) has been defined as the second differential of a Gaussian function and is the general form of a waveform that results from the application of a Gaussian impulse to an impulse radiating antenna or transducer system (Daniels, 2004).

Synthetic Data

In this part, GPR wavelet is assumed to be a Ricker wavelet with 1024 samples and center frequency of 200 MHz. The synthetic trace shown in Figure 1(a) is obtained by convolution of reflectivity model that consists of 10 spikes with the Ricker wavelet. The noise vector includes a signal with Gaussian random distribution signal-to-noise-ratio (SNR) of 15 db and some outliers have also been included. First spike in themodel represents ground reflection by strength amplitude and other spikes are indicative of differentlayers.

To test the functionality of GCV score, the generated trace has been deconvolved by assuming the original wavelet to be known. The GCV curve and the Mean Squre Error (MSE) as functions of iteration have been calculated and shown in Figure 2. The estimated reflectivity series (minimizer of the GCV score) are shown in Figure 1(b).

Field data and Computations

The GPR data was acquired near Talesh city and Caspian Sea coast (Iran) with antenna frequency of 250 MHz in one traverse with length of 50 m. Local information indicated that some excavation has occurred at the end of the profile (Figure 3).

The final estimated wavelet has been illustrated in figure 4. Now, with estimated wavelet the desired deconvolved is achievable.

The resulting GCV curves as a function of iteration for all GPR traces together are shown in figure 5. It is now to be seen if this selection could result in achieving a suitable deconvoled section or not.

It shows that average optimum iteration number for this data set is 46. By choosing outputs in proportion with iteration 46, deconvolved trace for input traces would be provided and then, the final section would be illustrated by considering all traces together. In acquisition fields, overburdened and underneath layer shows high damping because of clayey material and humidity. In 20 ns, ground reflection is clearly visible and the event above it, which has been removed, indicates the presence of direct wave, a linear phenomenon, the effects of which are deleted by algorithms. From 40 ns up to 80 ns, the presence of another
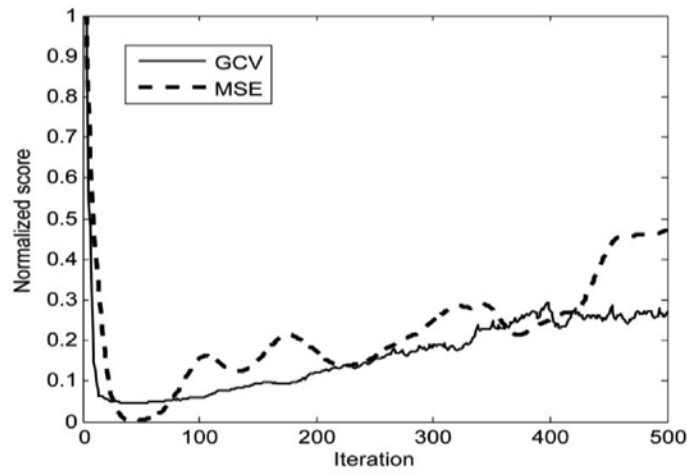
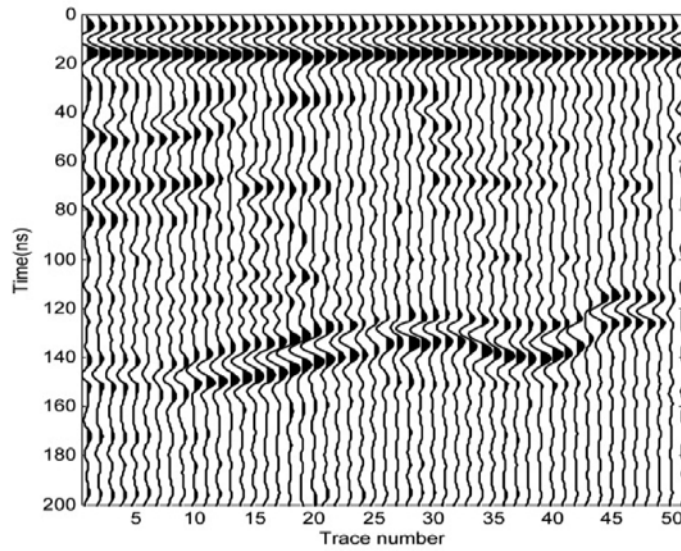**Figure 2.** Calculated GCV and MSE diagrams for synthetic trace.
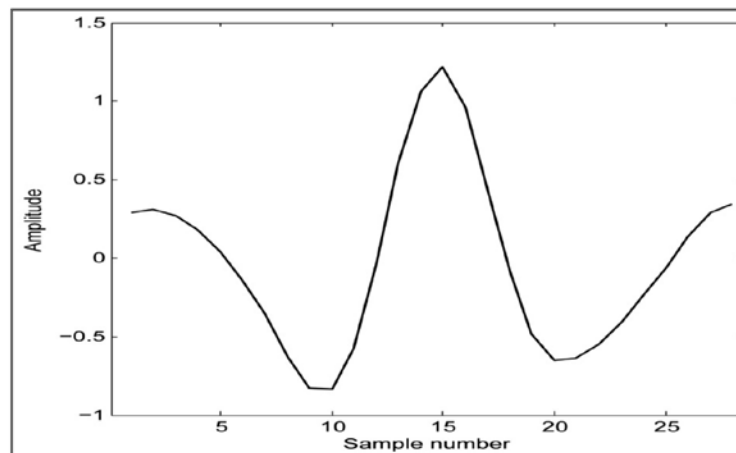

Figure 3. GPR section.

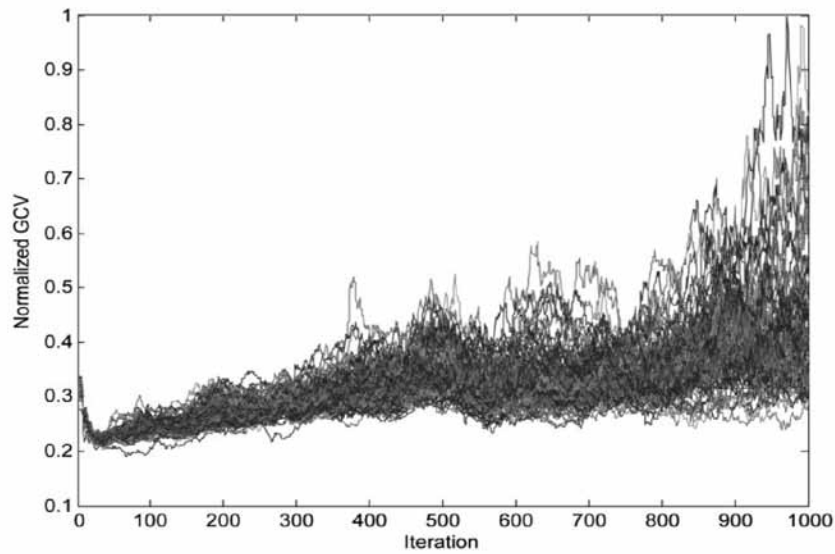**Figure 4.** The final estimated wavelet.

Figure 5. The resulting GCV curves with iteration corresponding to deconvolution of the GPR section shown in Figure 3.
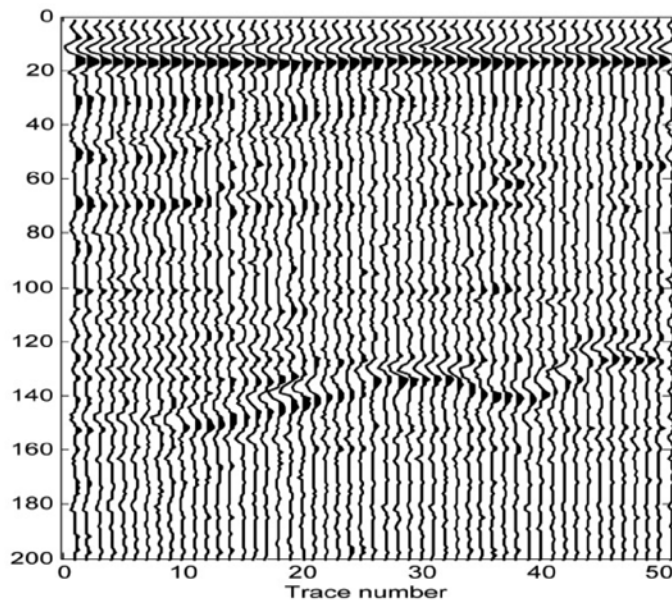

Figure 6. Deconvolved data section.

layer which seems to be narrower (tighter) deconvolved section is observed (Figure 6) compared to the raw section (Figure 3). Moreover, in120 ns up to 160 ns of the section, a reflection has occurred which is due to the excavation of multiple effects on top of it. The results show that the multiple effects have been suppressed. So, it appears that part of diffraction is reduced as shown in the last section in Figure 6 and the processed, compressed, signals compared to raw data (Figure 3).

CONCLUSIONS

Numerical experiments with synthetic and field GPR data confirmed that the proposed automatic deconvolution generates high-resolution estimators of the reflectivity in only a few iterations. It is thus recommended to be applied on similar GPR data. Moreover, the speed and quickness of achieving optimal results through the application of this algorithm makes it an efficient and accurate method for

delineation of very thin layers in GPR volumes. Attention must be paid to the fact that the algorithm is on the whole automatic without any requirementfor selecting parameters.

ACKNOWLEDGEMENTS

Compliance with Ethical Standards

The authors declare that they have no conflict of interest and adhere to copyright norms.

REFERENCES

Amundsen, L., 2001. Elimination of free-surface related multiples without need of the source wavelet, Geophys., v.66, no.1, pp: 327-341.

Baker, G. S., Steeples, D. W., Schmeissner, C., Pavlovic, M., and Plumb, R., 2001. Near surface imaging using coincident seismic and GPR data, Geophys. R. L., v.28, no.4, pp: 627-630.

Bano, M., Marquis, G., Niviere, B., Maurin, J., and Cushing, M., 2000. Investigating alluvial and tectonic features with ground-penetrating radar and analyzing diffractions patterns, Jour. of A.G., v.43, no.1, pp: 33-41.

Bednarczyk, Z., and Szynkiewicz, A., 2015. Applied Engineering Geology Methods for Exemplar Infrastructure Projects in Malopolskie and Podkarpackie Provinces. Springer International Publishing In Engineering Geology for Society and Territory, v.6, pp: 203-210.

Benedetto, A., Manacorda, G., Simi, A., and Tosti, F., 2002. Novel perspectives in bridges inspection using GPR, Nondestructive Testing and Evaluation, v.27, no.3, pp: 239-251.

Chahine, K., Baltazart, V., Dérobert, X., and Wang, Y., 2009. Blind deconvolution via independent component analysis for thin-pavement thickness estimation using GPR, Paper presented at the Radar Conference-Surveillance for a Safer World, 2009. RAD. Int.

Conyers, L.B., and Goodman, D., 1997. Ground-penetrating radar . An Introduction for Archaeologist. Alta. P., pp: 149-194.

Daniels, D.J., 2004. Ground penetrating radar., Iet., v.1.

Economou, N., and Vafidis, A., 2011. Deterministic deconvolution for GPR data in the tf domain, Near. S. G.,v.9, no.5, pp: 427-433.

Gholami, A., and Sacchi, M. D., 2012. A fast and automatic sparse deconvolution in the presence of outliers, Geoscience and Remote Sensing, IEEE. T.O., v.50, no.10, pp: 4105-4116.

Giannopoulos, A., 2005. Modelling ground penetrating radar by GprMax, Construc. and B.M., v.19, no.10, pp: 755-762.

Golub, G. H., Heath, M., and Wahba, G., 1979. Generalized cross-validation as a method for choosing a good ridge parameter, Techno., v.21, no.2, pp: 215-223.

Goodman, D., 1994. Ground-penetrating radar simulation in engineering and archaeology, Geophys., v.59, no.2, pp: 224-232.

Gottsche, F.-M., Stolte, C., and Nick, K.-P., 1994. Two-sided deconvolution-A Method to improve the temporal resolution in radar data, Paper presented at the 56th EAEG Meeting.

Hugenschmidt, J., 2002. Concrete bridge inspection with a mobile GPR system, Const. and B. M., v.16, no.3, pp: 147-154.

Irving, J., and Knight, R., 2006. Numerical modeling of ground-penetrating radar in 2-D using MATLAB. Comp. and Geosciences, v.32, no.9, pp: 1247-1258.

Jol, H.M. ed., 2008. Ground penetrating radar theory and applications. elsevier.

Jol, H. M., and Bristow, C. S., 2003. GPR in sediments: advice on data collection, basic processing and interpretation, a good practice guide, Geolog. S., London, Special Publications., v.211, no.1, pp: 9-27.

Li, L., 2014. Sparsity-promoted blind deconvolution of ground-penetrating radar (GPR) data, Geoscience and Remote Sensing Letters, IEEE., v.11, no.8, pp: 1330-1334.

Neves, F., Roulston, M., and Miller, J., 1995. Source signature deconvolution of ground penetrating radar data, Revis. B. G., v.13, no.2, pp: 143-153.

Ricker, N., 1953. The form and laws of propagation of seismic wavelets, Geophys., v.18, no.1, pp: 10-40.

Schmelzbach, C., Scherbaum, F., Tronicke, J., and Dietrich, P., 2011. Bayesian frequency-domain blind deconvolution of ground-penetrating radar data, Jour. of A.G., v.75, no.4, pp: 615-630.

Schmelzbach, C., and Huber, E., 2015. Efficient Deconvolution of Ground-Penetrating Radar Data, Geosc. and R. S., IEEE. T. O., v.53, no.9, pp: 5209-5217.

Sternberg, B. K., and McGill, J. W., 1995. Archaeology studies in southern Arizona using ground penetrating radar, Jour. of A. G., v.33, no.1, pp: 209-225.

Van Dam, R. L., and Schlager, W., 2000. Identifying causes of ground-penetrating radar reflections using time-domain reflectometry and sedimentological analyses, Sedimen., v.47, no.2, pp: 435-449.

Xia, J., Franseen, E. K., Miller, R. D., and Weis, T. V., 2004. Application of deterministic deconvolution of ground-penetrating radar data in a study of carbonate strata, Jour. of A.G., v.56, no.3, pp: 213-229.

Xia, J., Franseen, E. K., Miller, R. D., Weis, T. V., and Byrnes, A. P., 2003. Improving ground-penetrating radar data in sedimentary rocks using deterministic deconvolution, Jour. of A.G., v.54, no.1, pp: 15-33.

Yilmaz, Ö., 2001. Seismic data analysis . Tulsa, Soc. of Exploration Geophysicists, v.1, pp: 74170-2740.